The photodynamic activities of dimethyl 13[1]-[2-(guanidinyl)ethylamino] chlorin e_6 photosensitizers in A549 tumor

Ying-Hua Gao[1], Vanda Lovreković[2], Akmaral Kussayeva[2], Dan-Ye Chen[1], Davor Margetić[2]*, Zhi-Long Chen[1]*

[1] Department of Pharmaceutical Science & Technology, College of Chemistry and Biology, Donghua University, Shanghai 201620, China

[2] Division of Organic Chemistry and Biochemistry, Ruđer Bošković Institute, Bijenička c. 54, 10000, Croatia

* Corresponding authors:

Davor Margetić, E-mail: margetid@irb.hr

Zhi-Long Chen, E-mail: zlchen1967@qq.com

Abstract

Effective photosensitizers are particularly important factor in clinical photodynamic therapy (PDT). However, there is scarcity of photosensitizers for simultaneous cancer photo-diagnosis and targeted PDT. Herein, two novel dimethyl 2-(guanidinyl)ethylamino chlorin e_6 photosensitizers were synthesized and their efficacy in PDT in A549 tumor was investigated. It was showed that compounds **3** and **4** have a long absorption wavelength in the near infrared region and strong fluorescence emission with slow photo-bleaching rate and markedly strong ability of $^1O_2$ generation. They exhibited lower cytotoxicity and higher photo-cytotoxicity *in vitro* compared to the known anticancer drug *m*-THPC in MTT assay in A549 lung cancer cell lines. Compound **4** exhibit better inhibition effect than compound **3** and the IC_{50} value of compound **4** was 0.197 μM/L under 2 J/cm^2 laser irradiation, while compound **3** showed better anti-tumor effects compared to compound **4** *in vivo*. Intracellular ROS generation was found to be responsible for apoptotic cell death in DCFDA assay. Subcellular localization confirmed the damage site of compounds **3** and **4** in PDT. These findings suggest that the two novel photosensitizers might serve as potential photosensitizers for improved therapeutic efficiency of PDT.

Keywords: chlorin e_6 derivative; guanidine; photodynamic therapy; photosensitizers; reactive

oxygen species; tumor

Introduction

Guanidines are amongst the strongest organic bases in which after protonation, positive charge is stabilized by the resonance in the aromatic 6π-electron Y-delocalised system.[1] This capability ensures that the guanidine subunit is present in physiological conditions in its protonated form, thus increasing water solubility of the molecule. Described physicochemical properties make guanidine derivatives important in molecular recognition processes in biological systems, especially by acting *via* hydrogen bonding with carboxylates[2] and phosphates.[3] Compounds with guanidine functionalities are often potential drug candidates due to their ability to interact with many biological substrates and display interesting biochemical properties[4] including antimicrobial, antiviral and antitumor[5,6] activity. Of our particular interest are guanidine derivatives which were employed in photodynamic therapy (PDT)[7]. For instance, porphyrin guanidine and bisguanidine derivatives of the PDT agent verteporfin (Visudyne)[8] and guanidine and biguanide derivatives of tetraphenyl porphyrin[9] were prepared and showed an increased localization to the mitochondria with improved cytotoxicities. Our continued interest in the study of porphyrin-based PDT photosensitizers[10-13] led to the design of porphyrin derivatives with guanidinium mitochondria-targeting moieties, which at the same time introduce a positive charge and increase the hydrophilicity of the main compound.

PDT, as an emerging minimally invasive treatment modality for oncological and non-oncological applications is receiving more and more attention in clinical practice.[14] Singlet oxygen ($^1O_2$) is the major cytotoxic agent in most photosensitizers for clinical cancer treatment and also plays a critical role in treatment of various diseases.[15] For better cancer PDT, besides physicochemical properties, selectivity to carcinomas, specific subcellular organelle-targeting, and high cellular uptake are also required for photosensitizers.[16,17] Therefore, research of photosensitizer drugs that meet these requirements is essential for development of PDT.

Here we report the results of PDT antiproliferative activity of two novel chlorin e_6 guanidine conjugates which were designed to improve the mitochondrial targeting effects and increase the bioavailability.

Results and discussion

Synthesis

Chlorin-e_6 13^1-diaminoethylcarboxamide **2** was prepared by reaction of dimethyl pheophorbide a with ethylenediamine following the procedure of Smith *et al*.[18] (Scheme 1). When amine **2** was subjected to guanidinylation with 1*H*-pyrazole-1-carboxamidine reagent **6**, guanidine conjugate of chlorin e_6 **3** was obtained in 67 % yield. Guanidine conjugate **3** can also be prepared in two synthetic steps, by the guanidinylation/deprotection sequence. In this synthetic route, guanidinylation of amine **2** with *N*,*N*'-di-Boc-1*H*-pyrazole-1-carboxamidine reagent **7[**19**]** afforded *N*,*N*'-di-*tert*-butyloxycarbonylguanidine product **4** in 70 % yield. Deprotection of **4** was achieved by the employment of trifluoroacetic acid.[20]

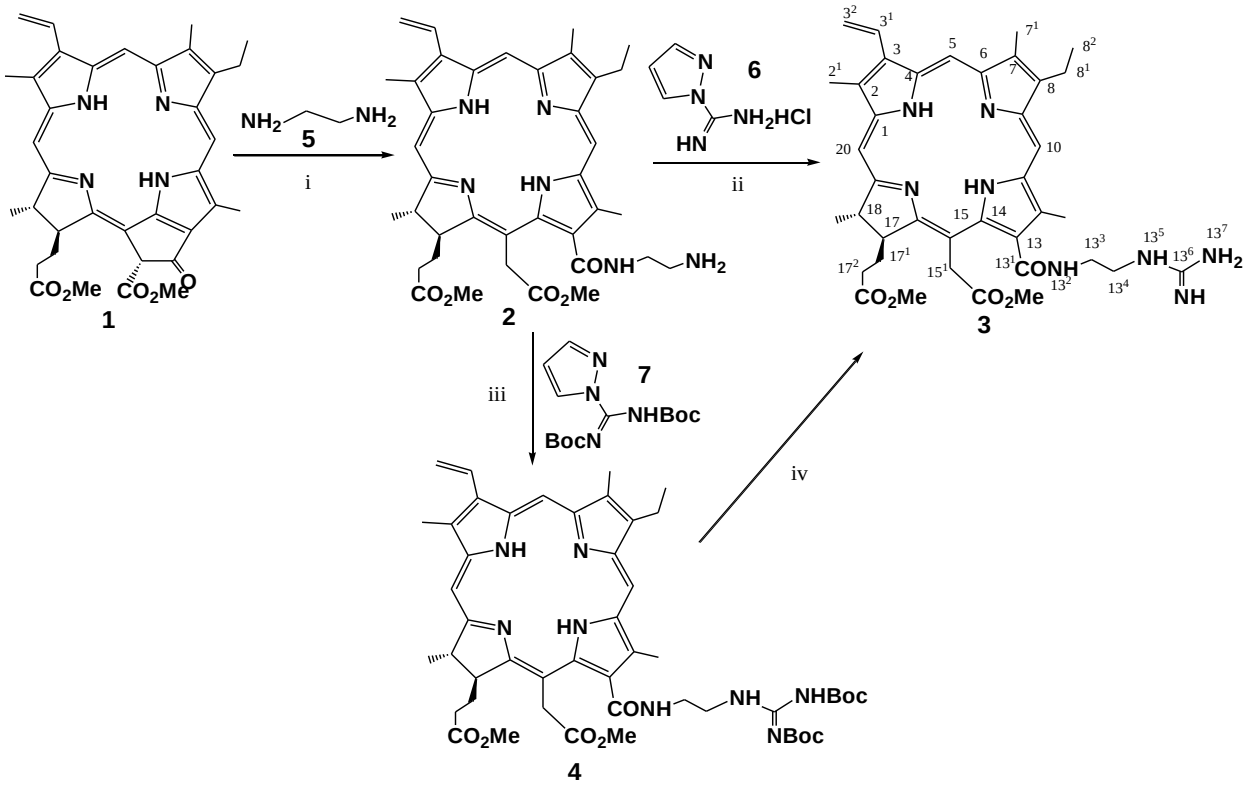

Scheme 1. Synthesis of **2**-**4**. Conditions: i) **5**, dry THF, RT, 24h, 44%, ii) **6**, DMF, DIEA, RT, 3d, 67 %, iii) **7**, DMF, DIEA, RT, 3d, 70%, iv) TFA, DCM, RT, 3h, 88%

Photophysical properties

Most porphyrin guanidine and bisguanidine derivatives have a strong absorbance at Q-band which enables excitation by long-wavelength light with high penetrability.[21,22] The UV-vis

absorption spectra of compound **3** and **4** were recorded in DMSO. The results showed that UV-vis spectrum of compound **3** was similar to compound **4**. Compounds **3** and **4** exhibit five distinct spectral peaks with maxima at 664, 608, 529, 501, and 403 for compound **3** and 664, 609, 529, 501, and 403 in compound **4**, respectively (**Fig. 1**). Molar extinction coefficients were calculated in **Table 1**.

As shown in **Fig. 2**, when compounds **3** and **4** were excited at wavelength of 400 nm, the maximum emission wavelength was 668 nm. Their fluorescence emission wavelength has red shift by 4 nm compared to maximum absorption wavelength. Fluorescence intensity of compound **4** was relatively higher than compound **3** (**Table1**). The results indicated that compounds can be used for further studies as pre-drugs for fluorescence diagnosis and photodynamic therapy.

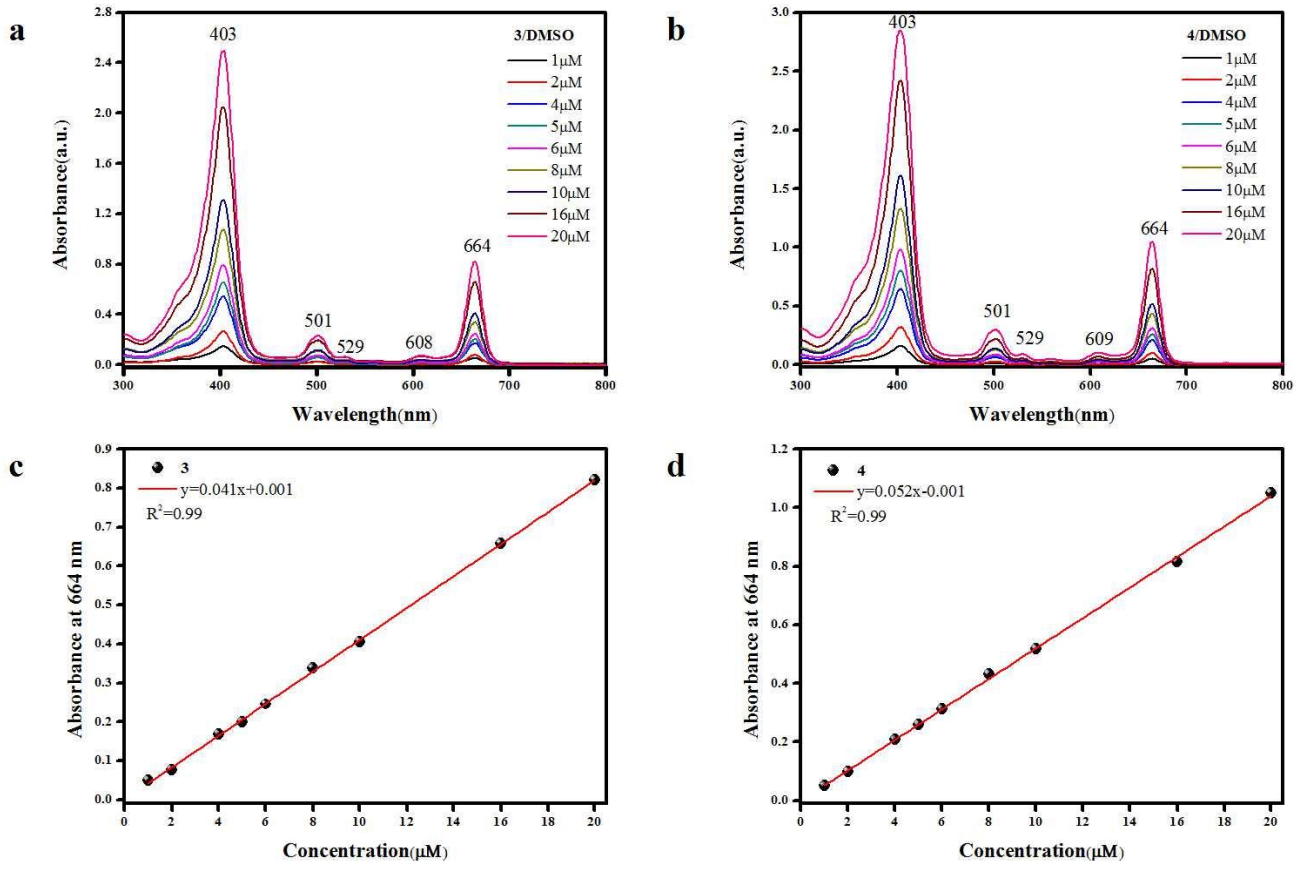

Fig. 1. (**a**) UV-vis absorption spectra of compounds **3** (1 - 20 μM) in DMSO, (**b**) UV-vis absorption spectra of **4** (1 - 20 μM) in DMSO. (**c**, **d**) The linear relationship between concentration and absorbance of compound **3** and **4** at 664 nm.

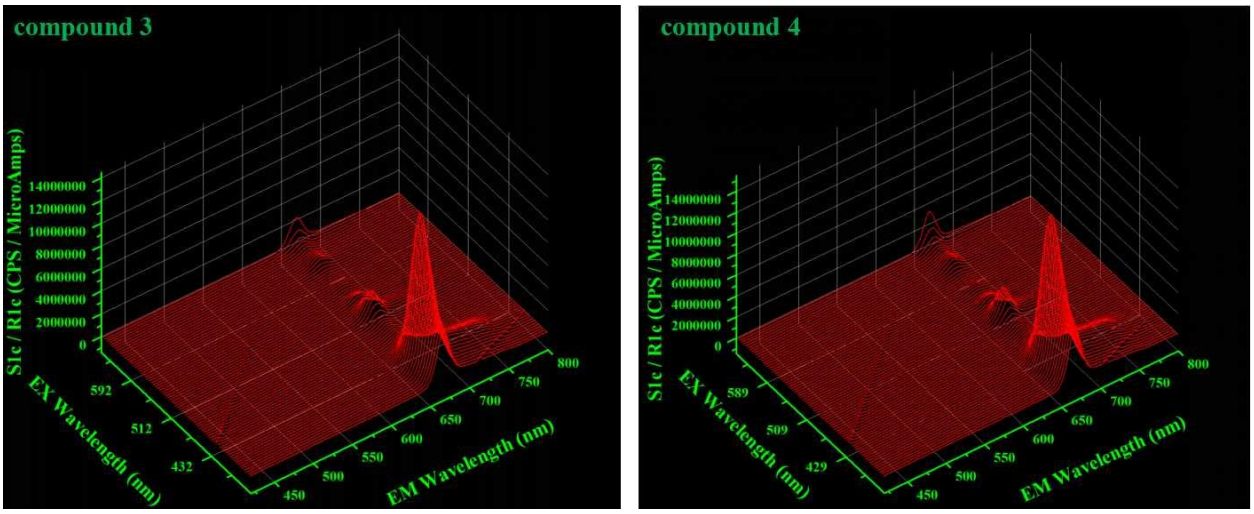

Fig. 2. The 3D fluorescence spectra of compounds **3** and **4** (5 μM) in DMSO.

Photochemical properties

Singlet oxygen is the main toxicity agent and the main cause of photo-bleaching, hence monitoring of photo-bleaching could provide a quantifiable measure of the singlet oxygen production.[23] Under 650 nm laser irradiation, the absorbance of compounds **3** and **4** decreases little (**Fig. 3a** and **3b**). They exhibited lower photo-bleaching rate (**Fig. 3c**). This indicated that compounds **3** and **4** were sufficiently stable under laser irradiation in the medium. Among all ROS, singlet oxygen ($^1O_2$) is widely concerned because of its high chemical reactivity derived from its characteristic electronically excited state.[24] Reactive oxygen species (ROS) plays an important role in cell signaling and stress response especially in the field of PDT for cancer treatment.[25] The practicability of DPBF to detect $^1O_2$ produced by compounds **3** and **4** were evaluated. The absorption intensity of the solution at 413 nm obviously decreased after each laser irradiation (**Fig. 3d** and **3e**). Compounds **3** and **4** have relatively higher ROS yields compared to *m*-THPC (0.47), among which **3** has the strongest ability to generate $^1O_2$ (**Fig. 3f** and **Table 1**).

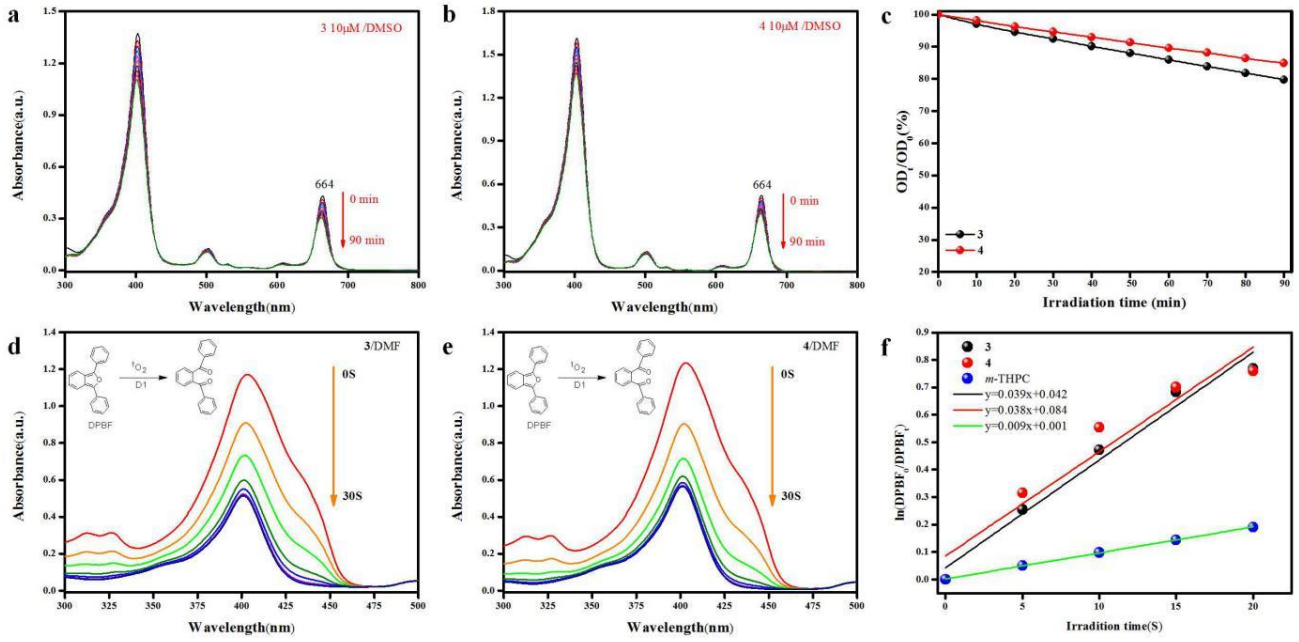

Fig. 3. Photochemical properties of photosensitizers. **(a)** Changes in absorption spectra of compound **3** at 650 nm. (**b**) Changes in absorption spectra of compound **4** at 650 nm. (**c**) Photobleaching rate of compounds **3** and **4**. (**d**) Photodecomposition of DPBF by $^1O_2$ after irradiation of compound **3** in DMF. (**e**) Photodecomposition of DPBF by $^1O_2$ after irradiation of compound **4** in DMF. (**f**) The plot for the generation rate of $^1O_2$ (**3**, **4,** *m*-THPC) in DMF.

Table 1. The absorption wavelength, the molar extinction coefficient ε, the fluorescence excitation and emission of compounds **3**, **4** and *m*-THPC; the generation rate (K) and yields (Φ_Δ) of singlet oxygen.

compound	λ/Molar extinction coefficient ε[$M^{-1}\cdot cm^{-1}$]	Excitation λ(nm)	Emission λ(nm)	S1c / R1c$_{max}$ (CPS / MicroAmps)	K[S^{-1}]	Φ_Δ
3	403(131000);501(11400);529(3000);608(3400);664(40600)	400	668	1.3072×10^7	0.039	2.03
4	403(161300);501(13600);529(3200);609(3800);664(51800)	400	668	1.3979×10^7	0.038	1.98
m-THPC	421(228100);520(18600);546(12300);598(7000);652(42800)	427	653	9.12×10^6	0.009	0.48

Cellular uptake and cytotoxicity assays *in vitro*

The cellular uptake of compounds **3** and **4** in A549 cells at various incubation times were also quantified (**Fig. 4a**). The intracellular concentrations of compounds **3** and **4** increased rapidly in the first 2 h, reached a plateau at about 12 h, and maintained within 24 h. The uptake amount of compound **4** was higher than compound **3**. This might suggest that the compounds can rapidly enter the cell through cell membrane.

Some research findings have suggested that the cytotoxic effect of the photosensitizer is basically due to the intrusion of photosensitizer in the cytoplasm and other organelles. Then photosensitizer could cause damage to the internal organelles of the cells and initiate different immunological reactions.[26,27] The cytotoxicity of the compounds **3** and **4** were evaluated against the A549 cells. As depicted in **Fig. 4**, compounds **3** and **4** were non-cytotoxic at low concentrations as *m*-THPC in the dark. As expected, the laser irradiation enhanced the photosensitizer effect for all samples loading compound compared with no laser irradiation. Meanwhile, compounds **3** and **4** indeed displayed an increased inhibition of cell growth in a concentration- and light-dose-dependent manner. Compounds **3** and **4** showed higher photo-toxicity compared to *m*-THPC under irradiation. When the dose of light was constant, the cell viability decreased as the drug concentration increased. Increased light dose at the same drug concentration, cell viability decreased. Under 2 J/cm^2 irradiation, the half-maximal inhibitory concentration (IC_{50}) of compound **3** was approximately 0.545 μM, while that of the compound **4** was 0.197 μM. Because of higher cellular uptakes of compound **4**, the IC_{50} values of compound **4** were lower than that of compound **3 (Table 2)**. The *in vitro* cytotoxicity results indicated that compounds **3** and **4** were effective in PDT and could be potent photosensitizers for PDT treatment.

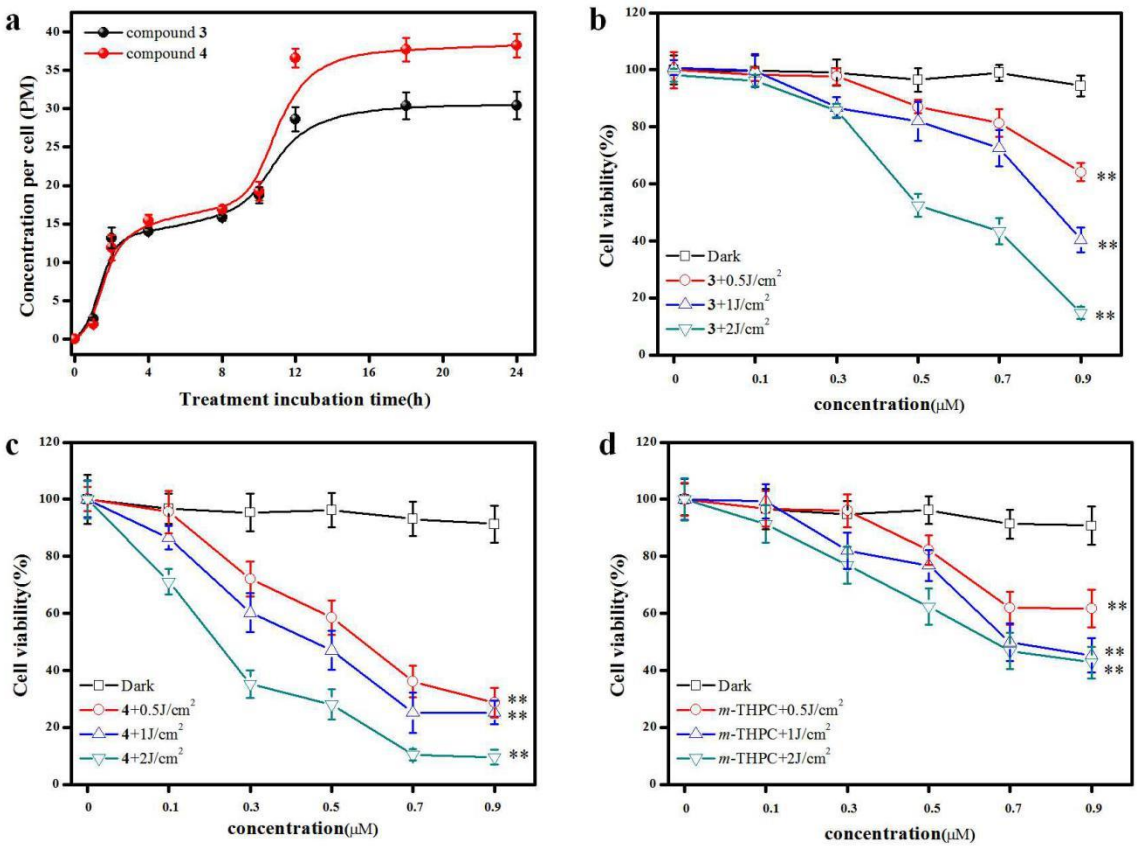

Fig. 4. (**a**) Intracellular accumulation of compounds **3** and **4**. (**b, c, d**) The cell viability of A549 cells treated by **3**, **4** and *m*-THPC at the concentrations of 0.1-0.9 μM with different light dose (dark, 0.5, 1, 2 J/cm^2) in MTT assay. ** P<0.01.

Table 2. The IC_{50} Values of compounds toward A549 Cells

Compound	IC_{50}(μM)		
	0.5 J/cm^2	1 J/cm^2	2 J/cm^2
3	1.264	0.886	0.545
4	0.542	0.397	0.197
m-THPC	1.099	0.779	0.702

Intracellular Reactive Oxygen Species (ROS) generation

The effect of compounds **3** and **4** on intracellular ROS generation was investigated by DCFH-DA dye as an indicator.[28,29] The dye cleaved by the intracellular esterase is converted into

highly fluorescent 2,7-dichlorofluorescein (DCF) on oxidation by intracellular ROS or ROS generated in situ, emitting green light.[30] The higher green fluorescence corresponded to the higher intracellular ROS generation. After incubating with 1 μM compound for 4 h and DCFH-DA for 20 min, the cells in PDT groups were irradiated with 650 nm laser (2 J/cm^2). As illustrated in **Fig. 5**, green fluorescence could be observed in PDT groups, while no fluorescence could be traced in other groups indicating that compounds **3** and **4** could generate ROS under laser irradiation. Compound **4** - PDT group exhibited a relative higher ROS generation in A549 cells compared to compound **3** - PDT group. We found that intracellular ROS generation was consistent with cytotoxic tests. These results indicated that the cytotoxicity of A549 cells after PDT was due to the generation of intracellular ROS.

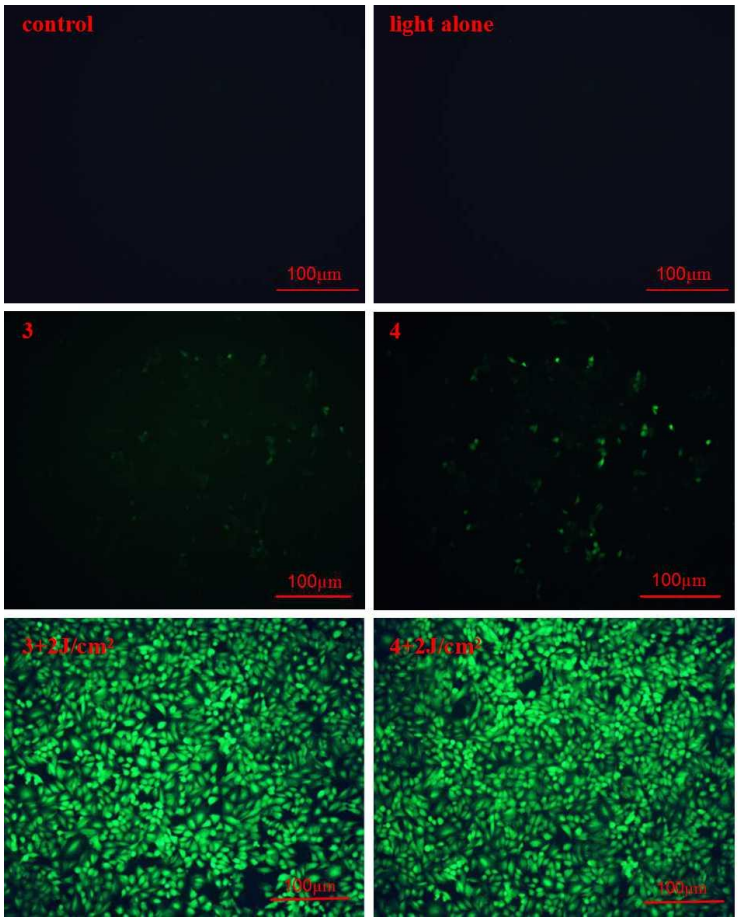

Fig. 5. The intracellular ROS generation induced by compounds **3** and **4** with 2 J/cm^2 650 nm laser in A549 cells detected by fluorescent microscopy (×200) with DCFH-DA as a probe. Scale bar: 100 μm.

Subcellular localization

Photodynamic therapy (PDT) involves a set of complex factors that include the photosensitizing agent, light, oxygen and various biological targets within the tissue.[31] Subcellular localization in A549 cells was investigated by confocal laser scanning microscopy.[32] A549 cells were incubated with compounds for 4 h, and then subcellular organelle was labeled with Mito-Tracker Green (MTG), Lyso-Tracker Blue (LTB), and ER-Tracker Green (ETG) before the imaging experiment, respectively. Fig. **6** demonstrated that the red fluorescence of compounds **3** and **4** overlapped with Mito-Tracker Green, Lyso-Tracker Blue, and ER-Tracker Green[DiOC6(3)], indicating that compounds **3** and **4** were accumulated and localized in mitochondria, lysosome and endoplasmic reticula. These results promise an enhanced performance of PDT.

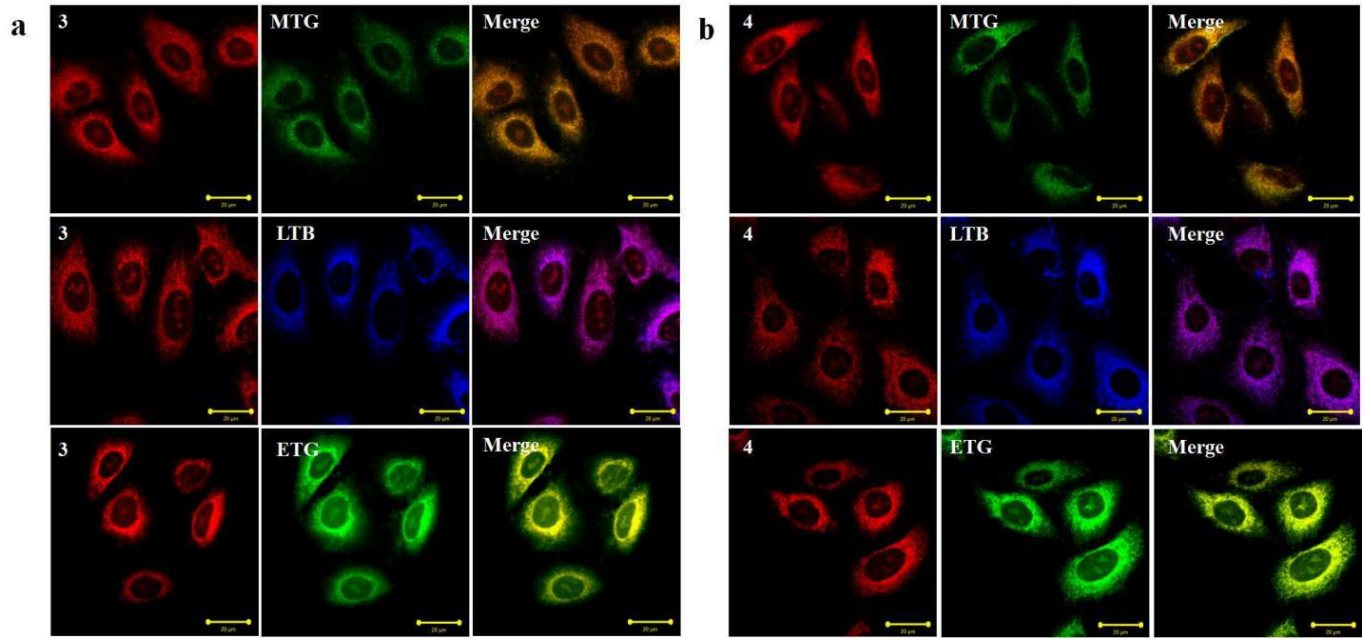

Fig. 6. The subcellular localization in A549 cells co-stained with Mito-Tracker, Lyso-Tracker, and ER-Tracker. Scale bar: 20 μm.

Therapeutic effects of the photosensitizers *in vivo*

Next, the efficacy of the photosensitizer drugs for PDT against A549 tumor in Balb/c nude model was assessed. This type of tumor is associated with poor prognosis and is difficult to cure. Therefore, we hoped to find effective photosensitizer to inhibit tumor growth. This experiment was divided into low dose group (0.15 mg/kg) and high dose group (0.4 mg/kg). The compound was injected intravenously into mice and irradiation with a 650 nm laser at tumor site. The images of tumors changes were recorded (**Fig. 7**). We found that the tumor growth in PDT group was relatively slower than in the control group. Tumor growth in drug alone group was same as the control group. Meanwhile, the therapeutic effect was evaluated by monitoring the tumor volume (**Fig.s 8a** and **8b**). After 13 d post-PDT, the A549 tumor was ablated and weighed (**Fig. 9**). The tumors in the PDT group were significantly smaller than the control and positive drug

groups at 0.15 mg/kg dose. At the low dose, compound **3**-PDT group has a better tumor inhibition than the compound **4**-PDT group. At the dose of 0.4 mg/kg, the tumors in the compound **3**-PDT and compound **4**-PDT groups were completely inhibited. The activity decrease of compound **4** compared with **3** in vivo may be caused by the introduction of two boc groups which increased the molecular weight related to the calculation of the administration dosage, and the boc groups could be removed during delivery in blood system and in the week acid tumor microenvironment.

In addition, tumors were dissected and histopathological examination (H & E) and TUNEL at 24 h after treatment was carried out. The tumor treated with the compounds under irradiation exhibited a wide range of tissue damage in histological sections, while most tumor cells showed no obvious change in the other groups. The cells showed apoptosis (green fluorescence) and necrosis in PDT groups (**Fig. 10**). These results indicated that compounds **3** and **4** were effective for A549 cancer in PDT.

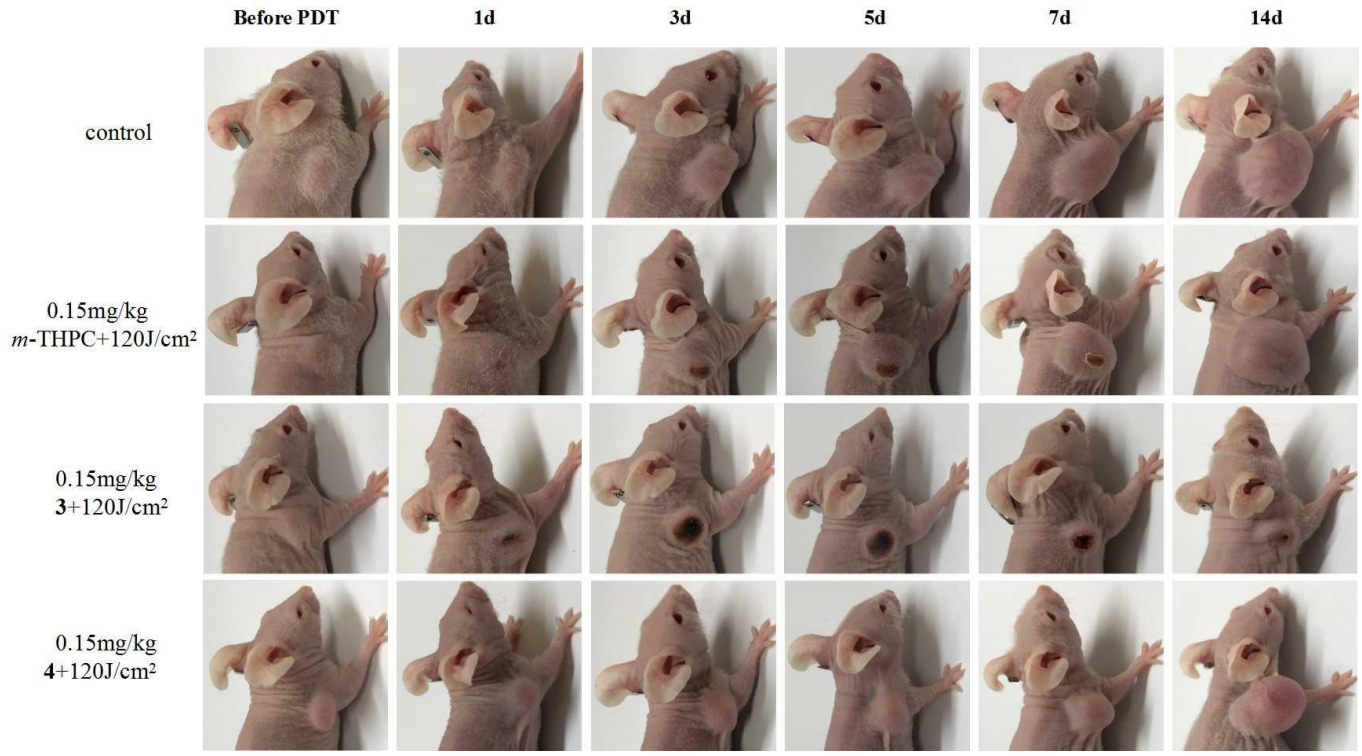

Fig. 7. PDT efficacy of 0.15 mg/kg compounds **3**, **4** in A549 tumor-bearing BABL/c nude mice.

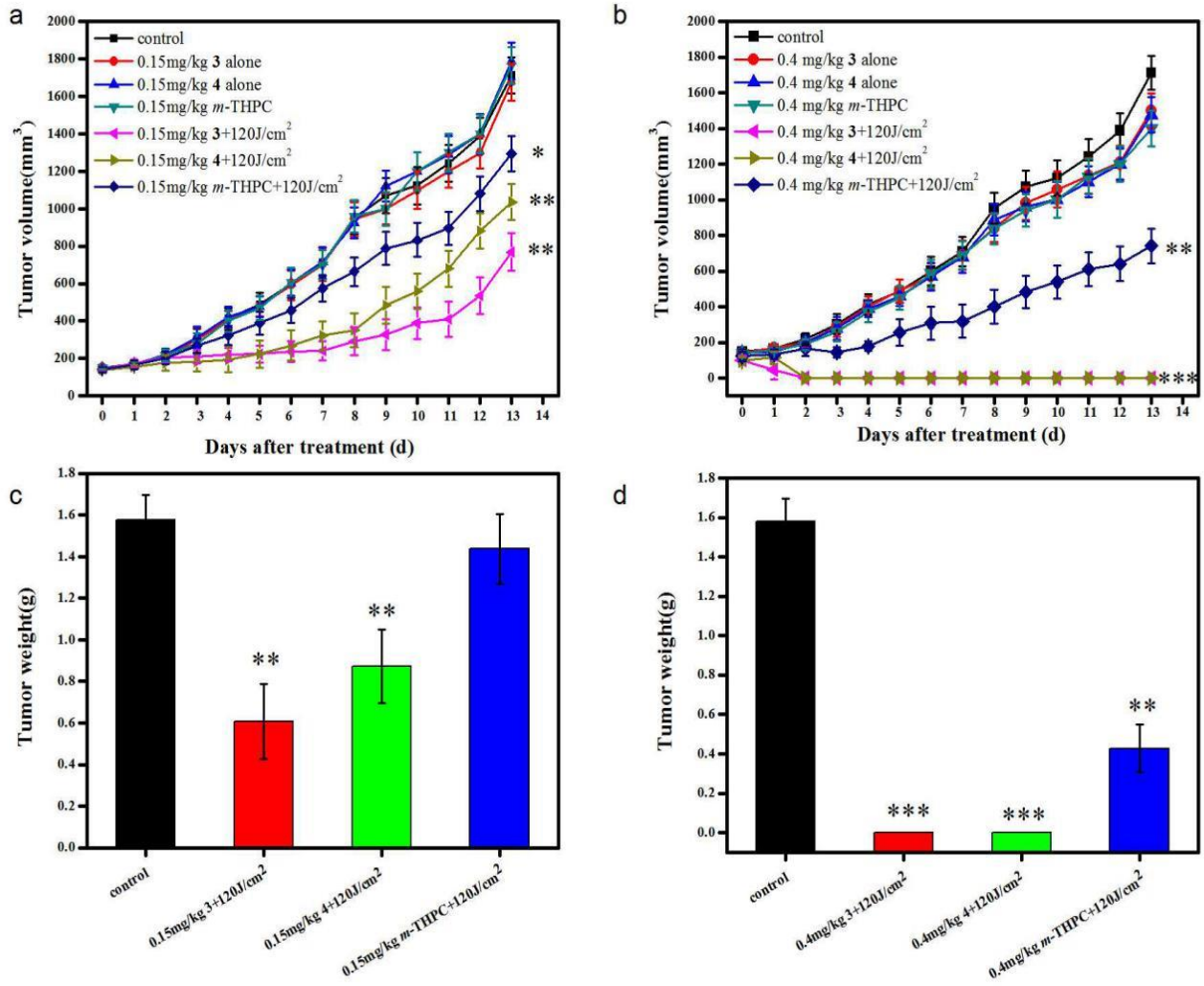

Fig. 8. (**a**) Tumor volume at different time points after 0.15 mg/kg compounds (**3**, **4**, *m*-THPC) treatment, (**b**) Tumor volume at different time points after 0.4 mg/kg compounds (**3**, **4**, *m*-THPC) treatment, (**c**) tumor weight at 13 d post PDT (0.15 mg/kg compounds), (**d**) tumor weight at 13 d post PDT (0.4 mg/kg compounds). **P<0.01, ***P<0.001.

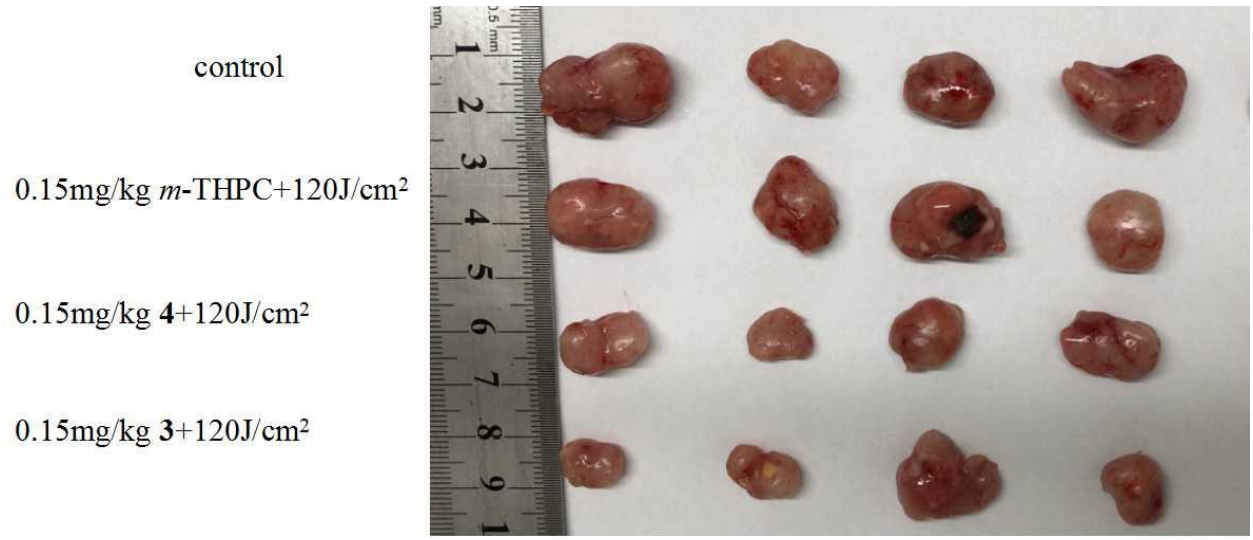

Fig. 9. Images of A549 tumor at 13 days after PDT.

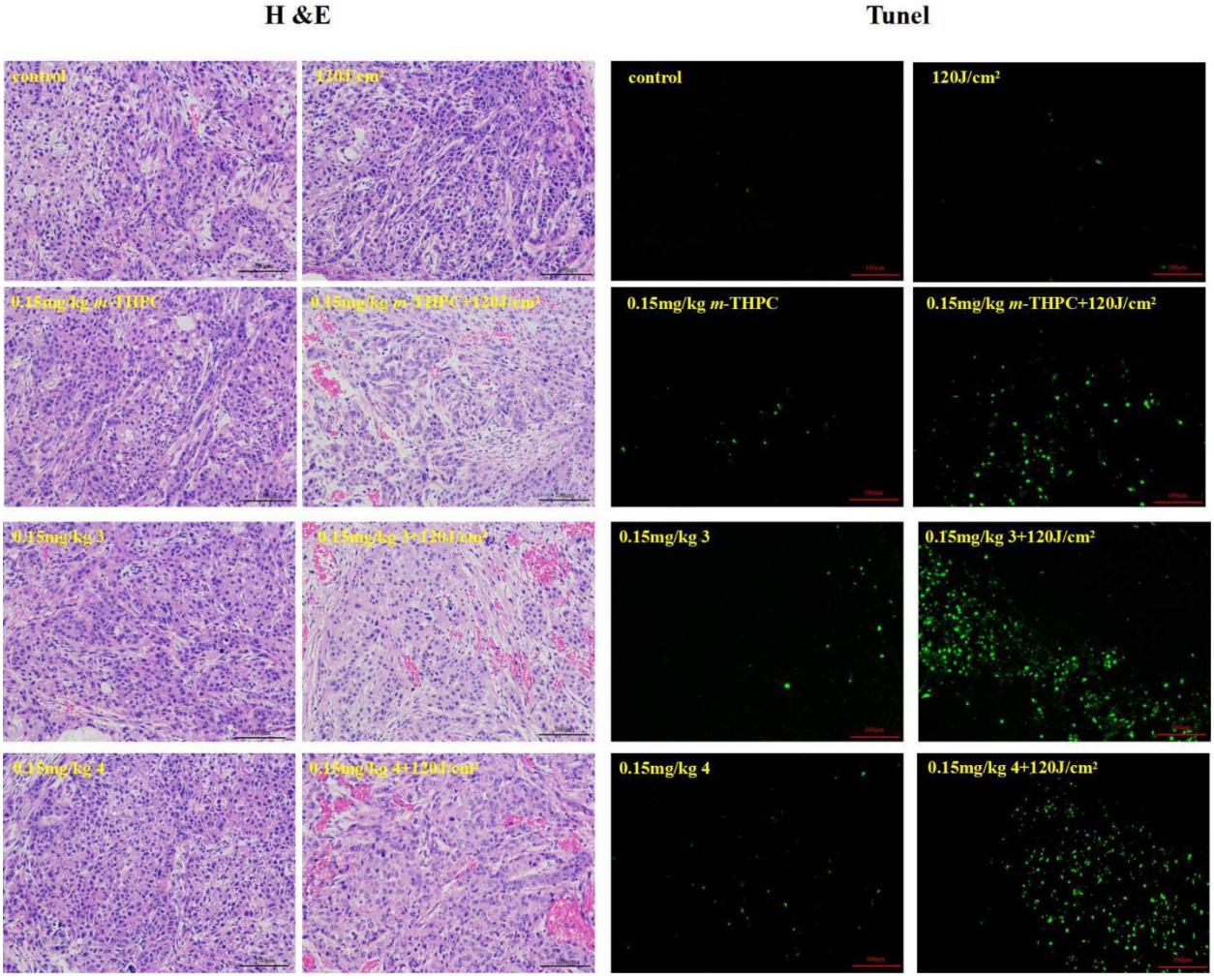

Fig. 10. Representative H&E and TUNEL images of PDT treated tumors under various conditions (control; light alone; drug alone and the PDT group, light dose 120 J/cm^2, 650 nm).

Conclusions

In summary, two novel dimethyl 2-(guanidinyl)ethylamino chlorin e_6 photosensitizers were synthesized and their efficacy in photodynamic therapy in A549 tumor was investigated. Absorptions of compounds **3** and **4** were in the near infrared region with the absorption maximum at 664 nm and fluorescence emission at 668 nm, their fluorescence emission have red shift by 4 nm. The new compounds were able to significantly elevate the $^1O_2$ generation compared to *m*-THPC (0.47). In the photo-bleaching experiment, compounds **3** and **4** exhibited lower photo-bleaching rate. Besides, compound **4** showed the highest intracellular accumulation and intracellular ROS. In vitro, compounds **3** and **4** exhibited higher photo-toxicity and lower dark toxicity than *m*-THPC to tumor cells. In view of their good performance, compounds **3** and **4** were selected to proceed with further PDT in vivo experimentation. Interestingly, compound **3** showed better tumor inhibition than compound **4**. This might be related to the metabolism of compounds in the mice. Subcellular localization confirmed that compounds **3** and **4** induced severe intracellular, oxidative, photodynamic damage in lung-cancer cells through the destruction of cellular organelles such as mitochondria, lysosomal and endoplasmic reticulum. Therefore, compounds **3** and **4** might be potential photosensitizers for the photodiagnosis and photodynamic therapy of cancer.

Supplementary material

Materials and methods as well as synthetic details for compounds **3** and **4** (experimental procedures and spectroscopic characterization) are given in Supplementary material.

Acknowledgments

This work was supported by the Croatian Science Foundation (grant No. IP-2018-01-3298, project Cycloaddition strategies towards polycyclic guanidines (CycloGu); Foundation of Shanghai Science and Technology Committee (No. 17430711900, 18430713000, 17PJ1432800, 17431902600, 17430741800, 18411968000, 18410721700，18430731600); Fundamental Research Fund for the Central Universities (No. 17D110513); The National Natural Science Foundation of China (No. 21372042).

References and notes

[1] Margetić, D. Physico-chemical properties of organosuperbases, in: Ishikawa, T. (Ed.), Superbases for Organic Synthesis: Guanidines, Amidines, Phosphazenes and Related Organocatalysts, Wiley, Chichester **2009**, pp. 9 - 48.

[2] Antol, I.; Glasovac, Z.; Margetić, D.; Crespo-Otero, R.; Barbatti, M. Insights on the auxochromic properties of guanidinium group. *J. Phys. Chem. A.,* **2016**, *120*, 7088 - 7100.

[3] Onda, M.; Yoshihara, K.; Koyano, H.; Ariga, K.; Kunitake T. Molecular recognition of nucleotides by the guanidinium unit at the surface of aqueous micelles and bilayers. A comparison of microscopic and macroscopic interfaces. *J. Am. Chem. Soc.*, **1996**, *118*, 8524 - 8530.

[4] Saczewski, F.; Balewski, Ł. Biological activities of guanidine compounds. *Expert Opin. Ther. Pat.* **2009**, *19*, 1417 - 1448.

[5] Andreani, A.; Burnelli, S.; Granaiola, M.; Leoni, A.; Locatelli, A.; Morigi, R.; Rambaldi, M.; Varoli, L.; Farruggia, G.; Stefanelli, C.; Masotti, L.; Kunkel, M. W. Synthesis and antitumor activity of guanylhydrazones from 6-(2,4-dichloro-5-nitrophenyl)imidazo[2,1-*b*]thiazoles and 6-pyridylimidazo[2,1-*b*]thiazoles. *J. Med. Chem.*, **2006**, *49*, 7897 - 7901.

[6] Ohara, K.; Smietana, M.; Restouin, A.; Mollard, S.; Borg, J.-P.; Collette, Y.; Vasseur, J.-J. Amine-guanidine switch: A promising approach to improve DNA binding and antiproliferative activities. *J. Med. Chem*. **2007**, *50*, 6465 - 6475.

[7] Zhou, J.; Mohamed, A. R. M.; Ma, S.; He, Y.; Yue, D.; Tang, J. Z.; Gu, Z. Tailoring the supramolecular structure of guanidinylated pullulan toward enhanced genetic photodynamic therapy. *Biomacromolecules,* **2018**, *19*, 2214 - 2226.

[8] Mahalingam, S. M.; Ordaz J. D.; Low, P. S. Targeting of a photosensitizer to the mitochondrion enhances the potency of photodynamic therapy. *ACS Omega*, **2018**, *3*, 6066 - 6074.

[9] Sibrian-Vazquez, M.; Nesterova, I. V.; Jensen, T. J.; Vicente, M. G. H. Mitochondria targeting by guanidine- and biguanidine-porphyrin photosensitizers. *Bioconjugate Chem.*, **2008**, *19*, 705 - 713.

[10] Srdanović, S.; Gao, Y.-H.; Chen, D.-Y.; Yan, Y.-J.; Margetić, D.; Chen, Z.-L. The photodynamic activity of 13^1-[2'-(2-pyridyl)ethylamine] chlorin e_6 photosensitizer in human esophageal cancer. *Bioorg. Med. Chem. Lett.,* **2018**, *28*, 1785 - 1791.

[11] Zhang, L. J.; Yan, Y.-J.; Liao, P. Y.; Margetić, D.; Wang, L.; Chen, Z.-L. Synthesis and antitumor activity evaluation of a novel porphyrin derivative for photodynamic therapy *in vitro* and *in vivo*. *Tumor Biol.,* **2016**, *37*, 6923-6933.

[12] Li, J.-W.; Wu, Z.-M.; Margetić, D.; Zhang, L.-J.; Chen, Z.-L. Antitumor effects evaluation of a novel porphyrin derivative in photodynamic therapy. *Tumor Biol.* , **2015**, *36*, 9685 - 9692.

[13] Briš, A.; Marinić, Ž.; Chen, Z.-L.; Margetić, D. Synthesis of chlorins by Diels-Alder cycloadditions of pheophorbide a and its derivatives. *Synlett,* **2015**, *26*, 991 - 994.

[14] Li, B. H.; Lin, L. S.; Lin, H. Y.; Wilson, B. C. Photosensitized singlet oxygen generation and detection: Recent advances and future perspectives in cancer photodynamic therapy. *J. Biophotonics,* **2016**, *11-12*, 1314 - 1325.

[15] Marydasan, B.; Madhuri, B.; Cherukommu, S.; Jose, J.; Viji, M.; Karunakaran, S. C.; Chandrashekar, T. K.; Rao, K. S.; Rao, C. M.; Ramaiah, D. In vitro and In vivo

demonstration of human-ovarian-cancer necrosis through a water-soluble and near-infrared-absorbing chlorin. *J. Med. Chem.*, **2018**, *61*, 5009 - 5019.

[16] Zhou, Z.; Song, J.; Nie, L.; Chen, X. Reactive oxygen species generating systems meeting challenges of photodynamic cancer therapy. *Chem. Soc. Rev.*, **2016**, *45*, 6597-6626.

[17] Bian, Y.; Li, M.; Fan, J.; Du, J.; Long, S.; Peng, X. A protonactivatable aminated-chrysophanol sensitizer for photodynamic therapy. *Dyes Pigm.*, **2017**, *147*, 476 - 483.

[18] Jinadasa, R. G. W.; Hu, X.; Vicente, M. G. H., Smith, K. M. Synthesis and cellular investigations of 17^3-, 15^2- and 13^1- amino acid derivatives of chlorin e_6. *J. Med. Chem.*, **2011**, *54*, 7464 - 7476.

[19] Đud, M.; Glasovac, Z.; Margetić, D. The utilization of ball-milling in synthesis of aryl guanidines through guanidinylation and *N*-Boc-deprotection sequence. *Tetrahedron,* **2019**, *75*, 109-115.

[20] Journigan, V. B.; Mésangeau, C.; Vyas, N.; Eans, S. O.; Cutler, S. J.; McLaughlin, J. P.; Mollereau, C.; McCurdy, C. R. Nonpeptide small molecule agonist and antagonist original leads for neuropeptide FF1 and FF2 receptors. *J. Med. Chem.*, **2014**, *57*, 8903-8927.

[21] Jain, M.; Zellweger, M.; Frobert, A.; Valentin, J.; van den Bergh, H.; Wagnieres, G.; Cook, S.; Giraud, M. N. Intra-arterial drug and light delivery for photodynamic therapy using Visudyne®: Implication for atherosclerotic plaque treatment. *Front. Physiol*., **2016**, *7*, 400. doi.org/10.3389/fphys.2016.00400.

[22] Rizvi, I.; Nath, S.; Obaid, G.; Ruhi, M. K.; Moore, K.; Bano, S.; Kessel, D.; Hasan, T. A. Combination of Visudyne and a lipid-anchored liposomal formulation of benzoporphyrin derivative enhances photodynamic therapy efficacy in a 3D model for ovarian cancer. *Photochem. Photobiol.*, **2019**, *95*, 419 - 429.

[23] James, N. S.; Cheruku, R. R.; Missert, J. R.; Sunar, U.; Pandey, R. K. Measurement of cyanine dye photobleaching in photosensitizer cyanine dye conjugates could help in optimizing light dosimetry for improved photodynamic therapy of cancer. *Molecules,* **2018**, *23*, 1842 - 1853.

[24] Wu, H. Y.; Song, Q. J.; Ran, G. X.; Lu, X. M.; Xu, B. G. Recent developments in the detection of singlet oxygen with molecular spectroscopic methods. *TrAC Trend. Anal. Chem.*, **2011**, *30*, 133-141.

[25] Tang, C. Y.; Wu, F. Y.; Yang, M. K.; Guo, Y. M.; Lu, G. H.; Yang, Y. H. A classic near-infrared probe indocyanine green for detecting singlet oxygen. *Int. J. Mol. Sci.*, **2016**, *17*, 219-226.

[26] Faedmaleki, F.; Shirazi, F. H.; Salarian, A.-A.; Ashtiani, H. A.; Rastegar, H. Toxicity effect of silver nanoparticles on mice liver primary cell culture and HepG2 cell line. *Iran. J. Pharm. Res.*, **2014**, *13*, 235 - 242.

[27] He, D.; Bligh, M. W.; Waite, T. D. Effects of aggregate structure on the dissolution kinetics of citrate-stabilized silver nanoparticles. *Environ. Sci. Technol.*, **2013**, *47*, 9148 - 9156.

[28] Li, K. T.; Chen, Q.; Wang, D. W.; Duan, Q. Q.; Tian, S.; He, J. W.; Ou, Y. S.; Bai, D. Q. Mitochondrial pathway and endoplasmic reticulum stress participate in the photosensitizing effectiveness of AE-PDT in MG63 cells. *Cancer Med.*, **2016**, *5*, 3186 - 3193.

[29] Huang, L. F.; Wei, G. F.; Sun, X. Q.; Jiang, Y. L.; Huang, Z. Q.; Huang, Y. J.; Xu, X. Y.; Shen, Y. F.; Liao, Y. H.; Zhao, C. S. A tumor-targeted Ganetespib-zinc phthalocyanine conjugate for synergistic chemo photodynamic therapy. *Eur. J. Med. Chem.*, **2018**, *151*, 294-303.

[30] Chanu, S. B.; Raza, M. K.; Banerjee, S.; Mina, P. R.; Musib, D.; Roy, M. ROS dependent antitumour activity of photo-activated iron(III) complexes of amino acids. *J. Chem. Sci.*, **2019**, *131*, 9. doi.org/10.1007/s12039-018-1584-3.

[31] Li, M. L.; Long, S. R.; Kang, Y.; Guo, L. Y.; Wang, J. Y.; Fan, J. L.; Du, J. J.; Peng, X. J. De novo design of phototheranostic sensitizers based on structure-inherent targeting for enhanced cancer ablation. *J. Am. Chem. Soc.*, **2018**, *140*, 15820 - 15826.

[32] Zou, J. H.; Wang, P.; Wang, Y.; Liu, G. Y.; Zhang, Y. W.; Zhang, Q.; Shao, J. J.; Si, W. L.; Huang, W.; Dong, X. C. Penetration depth tunable BODIPY derivatives for pH triggered enhanced photothermal/ photodynamic synergistic therapy. *Chem. Sci.*, **2019**, *10*, 268 - 276.